INTERSTELLAR GRAIN CHEMISTRY AND ORGANIC MOLECULES

L. J. Allamandola and S. A. Sandford,
NASA-Ames Research Center, Moffett Field, CA 94035

ABSTRACT

The detection of prominent infrared absorption bands at 3250, 2170, 2138, 1670 and 1470 cm^{-1} (3.08, 4.61, 4.677, 5.99 and 6.80 μm) associated with molecular clouds shows that mixed molecular ("icy") grain mantles are an important component of the interstellar dust in the dense interstellar medium. These ices, which contain many organic molecules, may also be the production site of the more complex organic grain mantles detected in the diffuse interstellar medium.

Theoretical calculations employing gas phase as well as grain surface reactions predict that the ices should be dominated only by the simple molecules H_2O, H_2CO, N_2, CO, O_2, NH_3, CH_4, possibly CH_3OH, and their deuterated counterparts. However, spectroscopic observations in the 2500-1250 cm^{-1} (4-8 μm) range show substantial variation from source to source, implying a far richer chemistry than expected from surface reactions alone. By comparing these astronomical spectra with the spectra of laboratory-produced analogs of interstellar ices, one can determine the composition and abundance of the materials frozen on the grains in dense clouds.

The 2170 cm^{-1} (4.61 μm) band is attributed to the CN stretching vibration in an unidentified grain constituent designated X(CN), while the 2138 cm^{-1} (4.677 μm) band is attributed to solid CO. Comparison of the CO band with laboratory data shows that there are two distinct chemical regimes in clouds, one dominated by atomic hydrogen, the other by molecular hydrogen.

The 1670 cm^{-1} (5.99 μm) feature is assigned primarily to the HOH bending mode in H_2O, in line with the identification of the 3250 cm^{-1} (3.08 μm) band as the OH stretching mode. Source-to-source variation on the high frequency side of this band is quite likely due to the C=O stretch in organic species such as ketones, aldehydes, esters, and carboxylic acids. The 1470 cm^{-1} band is largely due to the CH deformation modes, possibly in alcohols. The source-to-source variations in this band are probably due to differences in the amounts of unsaturated hydrocarbons, or saturated hydrocarbons which contain strongly electro-

negative groups, in different clouds. These variations suggest that energetic processing, such as by ultraviolet photolysis and cosmic ray bombardment, is important in determining the grain mantle composition.

In addition to reviewing the above, experiments are described in which the chemical evolution of an interstellar ice analog is determined during irradiation and subsequent warm-up. Particular attention is paid to the types of moderately complex organic materials produced during these experiments which are likely to be present in interstellar grains and cometary ices.

I. INTRODUCTION: CARBON AND ICY GRAIN MANTLES IN DENSE MOLECULAR CLOUDS

Dense interstellar clouds are comprised of gas and dust. The gas is a mixture of many different atoms, ions, radicals, and molecules. (see Irvine et al., 1985, and references therein). Interspersed with the gas, at lower abundance, are small, cold (~ 10 K) dust particles. The refractory component of these grains is thought to consist of silicates and amorphous carbon.

Because the grains are cold, most gaseous species (except H and H_2) striking the grains will stick, forming a mixed molecular ice mantle (see Greenberg, 1977, and references therein). The accreting species include atoms and radicals as well as molecules. At this point in our understanding of chemistry in clouds, two general types of molecular mantle are envisioned. One type is comprised largely of relatively simple species. The other consists of a chemically more complex mixture (Figure 1).

The simpler mantles are produced during the accretion of gas phase components. Chemical reactions, which are not possible in the gas phase, can occur between neighboring reactive components on grain surfaces during accretion. Consequently, the mantle will not simply reflect the gas phase composition, but can also contain other species. Since atomic H is very abundant during a significant fraction of a cloud's lifetime, atoms on the surface such as C, N, or O will quickly become hydrogenated and produce species such as CH_4, NH_3, and H_2O. Polar molecules such as H_2O and NH_3 will certainly remain on the surface and the mantle will become enriched in them. Non-polar molecules such as CH_4 may or may not stick upon formation. The first attempts to integrate gas and grain chemistry into a single model predicted that grain mantles produced in this way should fall into two categories depending on the H/H_2 ratio (Tielens and Hagen, 1982; d'Hendecourt, Allamandola, and Greenberg, 1985). If the H/H_2 ratio is large, reactions with H atoms are important and simple hydrides dominate the ice. If, on the other hand, it is substantially less than one, reactions involving species such as O and N become important and form molecules such as O_2 and N_2. Thus, two qualitatively different categories of mantle may be produced by grain surface reactions, one characterized by polar, H-bonded molecules and the other characterized by non-polar or only slightly polar, highly unsaturated molecules. Recently, more sophisticated models have been developed which examine the effects of additional surface reactions (Williams, 1987, 1988). Millar (1988) and Brown (1988), describe some of the more recent results using these models and show that slightly more complex species than simple hydrides, diatomics and triatomics can be produced by surface reactions.

Significantly more complex ice mantles should be produced by energetic processing with ultraviolet radiation and cosmic rays. In 1976 Greenberg suggested that the ultraviolet irradiation of grains in dense clouds would produce chemically complex molecules within ice

mantles. The photoproducts of irradiation span a broad range in number and complexity, starting with molecules as "simple" as CO_2 and H_2CO, and extending to large, poorly characterized species. As an example of the complexity in number, the many reaction pathways involving CO and the simple photoproducts of an ice made of H_2O, CH_4, and NH_3 is shown in Figure 2.

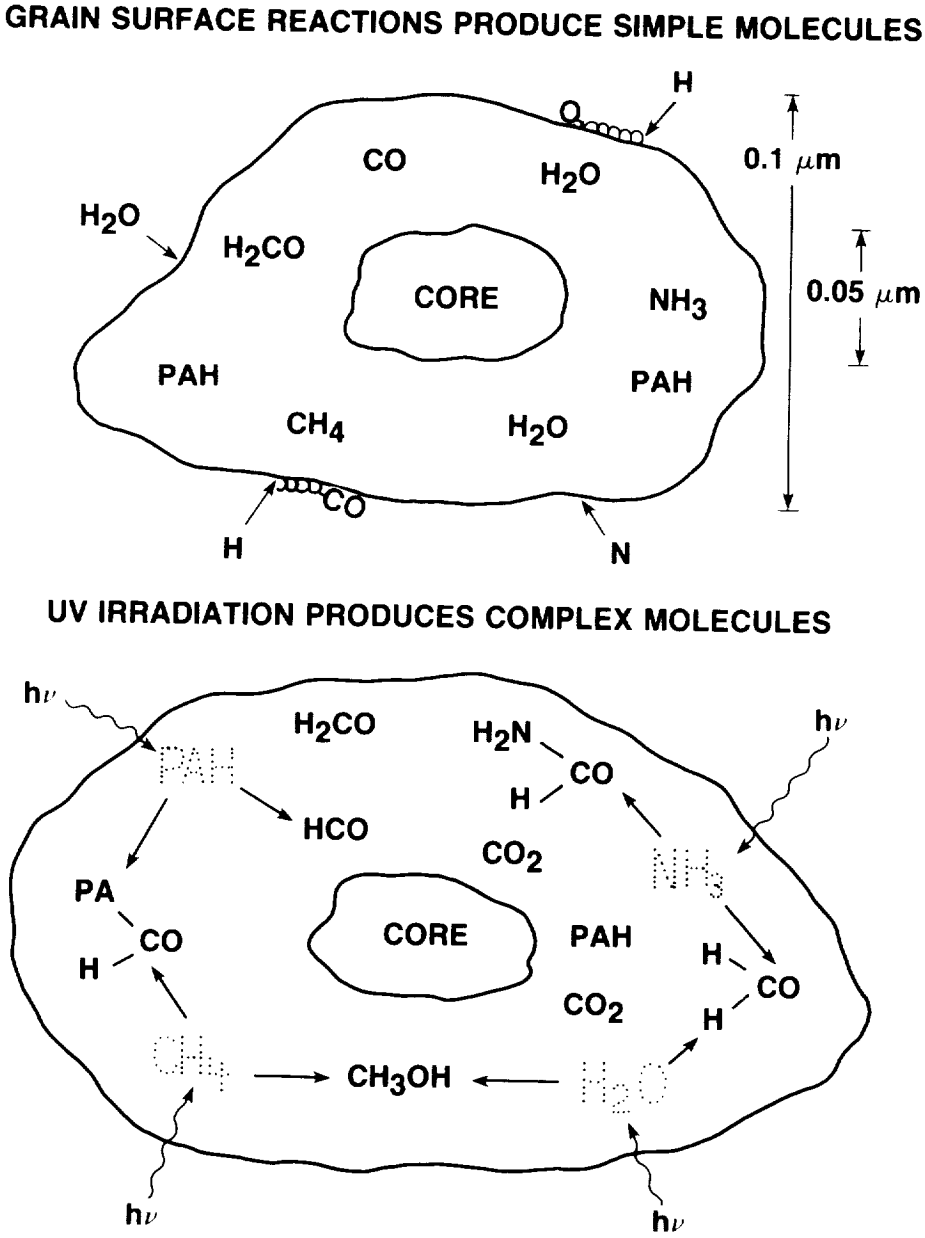

Fig. 1. Grain mantle growth and evolution.

Thanks to the development of powerful infrared observational tools and the persistence of infrared astronomers, high quality infrared spectra are available for a small number of sources in dense clouds. These spectra have revealed more about the composition of dust in molecular clouds than all of the previous observations combined because the infrared spectrum of a substance gives more information about its structure than any of its other properties (Figure 3). As discussed in the following sections, these spectra, interpreted in the light of laboratory analog experiments, are now beginning to provide compelling evidence for a broad range of organic molecules in grain mantles.

Sections II and III, which discuss ice analog production and the comparison of laboratory spectra with interstellar spectra, have been largely reproduced from Sandford and Allamandola, 1988. Sections IV and V discuss the photochemical and thermal evolution of ice analogs and astrophysical implications and are largely reproduced from Allamandola, Sandford and Valero, 1988.

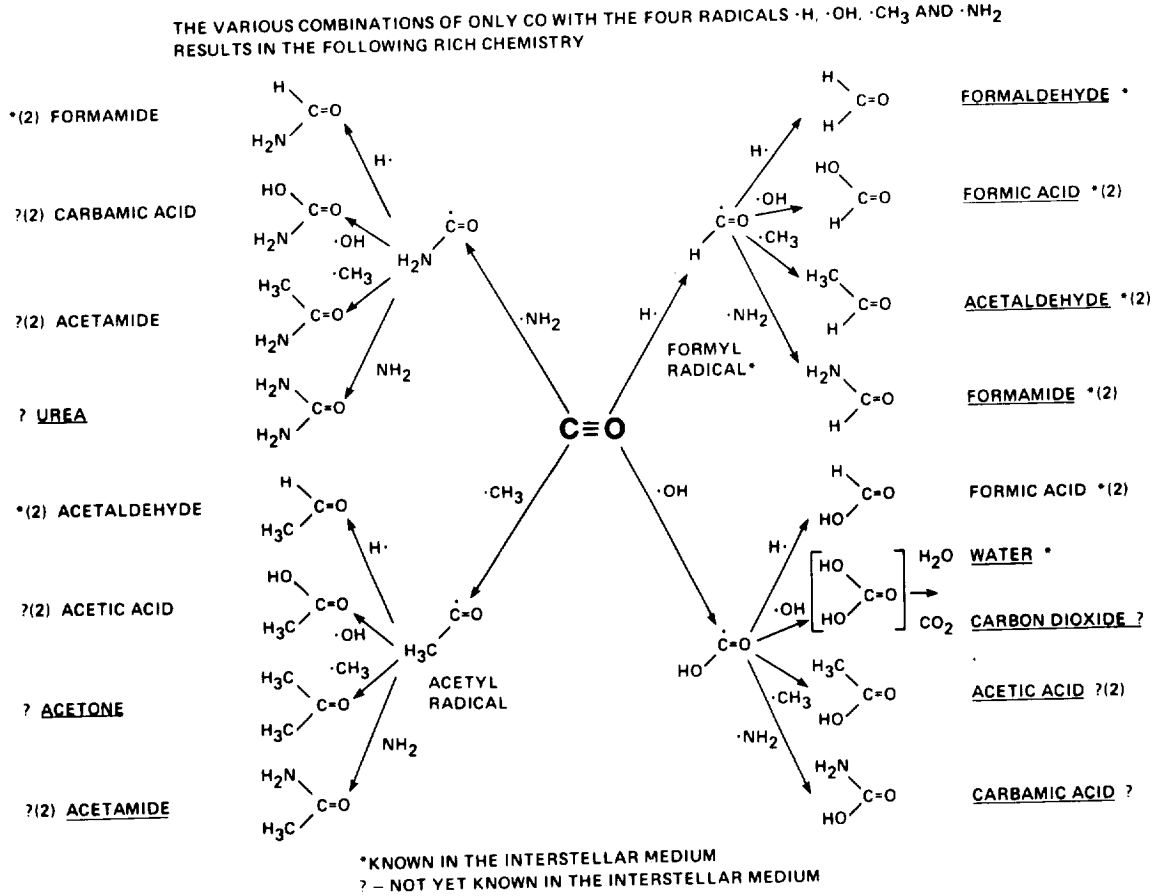

Fig. 2. Possible reaction pathways involving CO in an interstellar grain mantle illustrating how the intermediates H, OH, CH_3, and NH_2 can add to CO and produce a very rich chemical mixture.

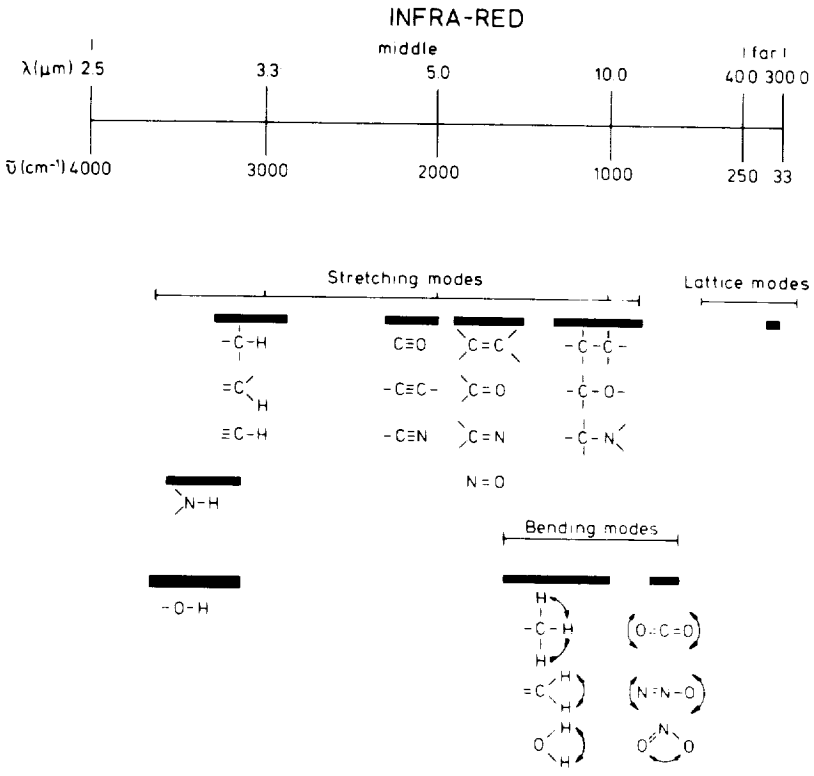

Fig. 3. Vibrational frequency ranges of various molecular groups.

II. INTERSTELLAR ICE ANALOG PRODUCTION

Mid-infrared absorption spectroscopy of ices in dense interstellar clouds generally depends on the presence of embedded or background radiation sources (Figure 4). Radiation from the source heats the immediately surrounding dust. This hot dust emits an infrared pseudo-blackbody continuum like that shown in the inset close to the protostar in Figure 4. As this radiation passes through the cloud, molecules along the line-of-sight absorb at their fundamental frequencies. This produces a spectrum which has absorption features diagnostic of the material along the line of sight (lower inset in Figure 4). Ice features generally dominate this type of absorption spectrum. The key features shown in Figure 4 (infrared source, absorbing material, and detection) must be mimicked in laboratory studies of ice analogs. The specific conditions within the cloud which must be duplicated to create interstellar ice analogs vary widely. Composition, temperature, and exposure to radiation can be duplicated reasonably well in the laboratory.

The general laboratory procedure consists of slowly flowing the gas from which the ice is made into a high-vacuum chamber. This gas, which can be a pure substance or a mixture of substances, is directed to and

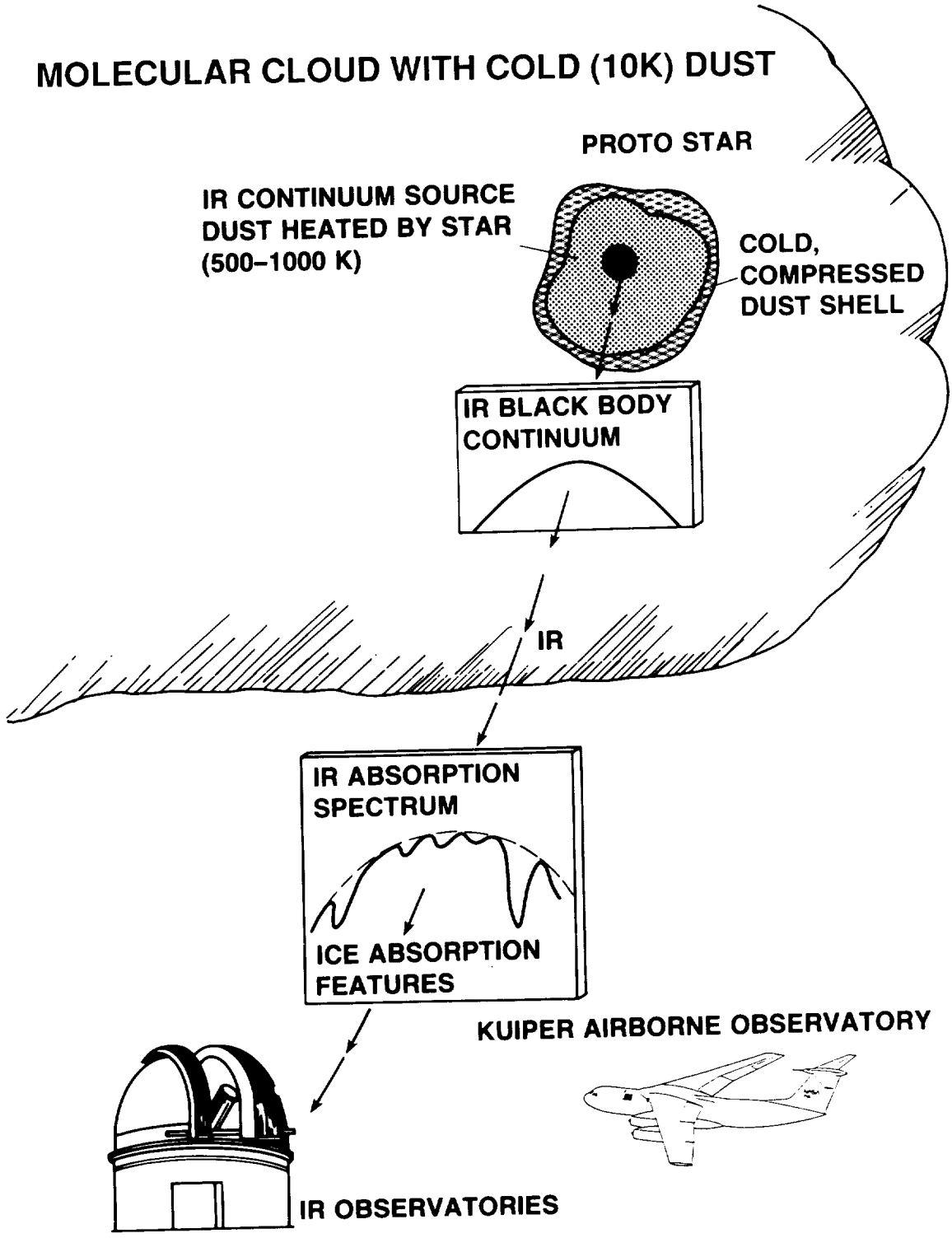

Fig. 4. Schematic illustration of how one obtains absorption spectra of interstellar ices.

condenses on the surface of a substrate cooled by a closed-cycle helium refrigerator or by a cryogen such as liquid helium. A schematic drawing of a typical sample chamber in various configurations is shown in Figure 5 and a photograph of the apparatus at Ames is given in Figure 6. Substrate temperature can generally be maintained anywhere from 10 K (4 K with liquid helium) to room temperature. The substrate is interchangeable. For infrared studies it is generally a cesium iodide window. The substrate is rotatable and is suspended in the center of a sample chamber with gas inlet tubes and several larger ports. The larger openings can be fitted with windows, lamps, ion sources, ovens, pressure gauges, mass spectrometers, phototubes, etc., depending upon the particular properties under study. Generally, the substrate is initially positioned to face the gas inlet tube for the preparation of the ice and then rotated to face the other ports as needed. Radiation processing of the sample can be carried out with ultraviolet lamps or ion sources. Subsequently, the evaporation characteristics of the ice can be studied by measuring spectra during warm-up of the substrate.

The column density of an individual component or molecular subgroup in an interstellar ice can only be determined for species in which the integrated absorbance, A, has been measured in the appropriate solid. The column density of any solid state species can be estimated by

$$N = \frac{\tau \Delta \upsilon_{\frac{1}{2}}}{A} \qquad (1)$$

where τ is the optical depth of the band at maximum absorbance, $\Delta\nu_{\frac{1}{2}}$ is the full-width-at-half-maximum in cm^{-1}, and A is the integrated absorbance in cm $molecule^{-1}$. The integrated absorbances for the vibrational transitions of a number of astrophysically interesting materials are listed in Table 1.

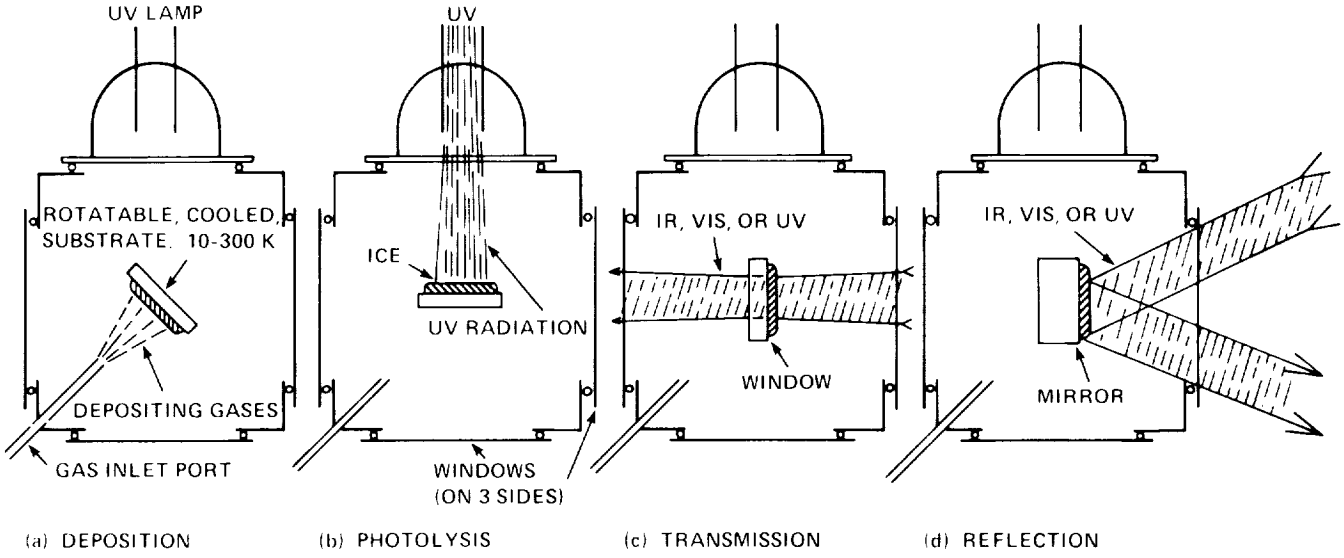

Fig. 5. Common configurations of a low temperature ice sample chamber.

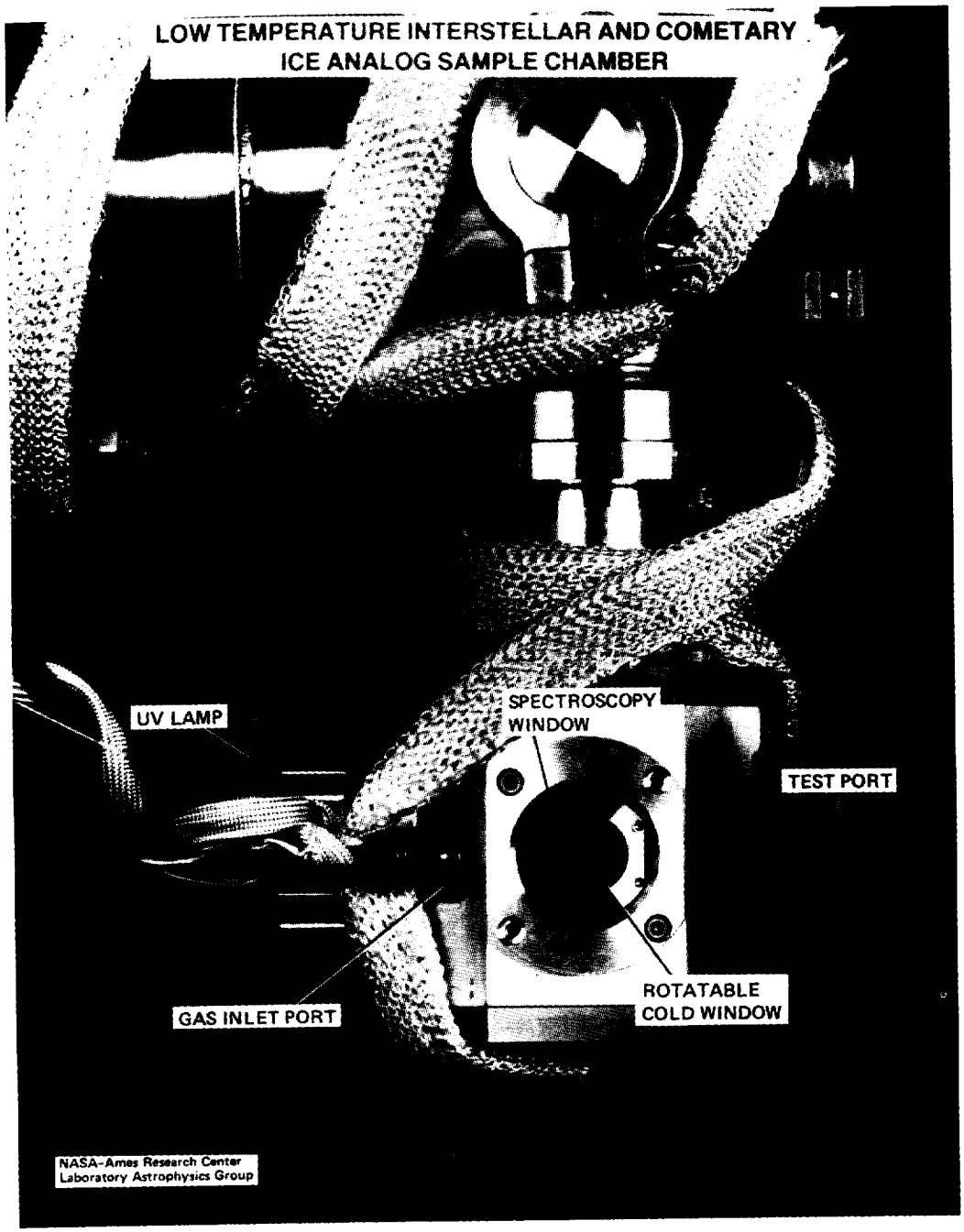

Fig. 6. Photograph of an Ice Analog sample chamber at NASA Ames Research Center. The base is approximately 10 cm on a side and the cold window is about 2 cm in diameter.

Table 1. Absorbance Values for Molecules in the Solid State

Molecule	Mode	Frequency (cm^{-1})	λ (μm)	A (cm/molecule)
H_2O[a]	OH-stretch	3275	3.053	2×10^{-16}
	OH-bend	1670	5.988	8×10^{-18}
	libration	750	13.33	3×10^{-17}
CO	stretch in CO[b]	2139	4.675	1×10^{-17}
	stretch in H_2O[c]	2137	4.680	2×10^{-17}
CO_2[c]	CO-stretch	2342	4.270	2×10^{-16}
	CO-bend	653	15.31	4×10^{-17}
CH_4[d]	CH-stretch	3010	3.322	6×10^{-18}
	CH-deformation	1300	7.692	6×10^{-18}
NH_3[d]	NH-stretch	3375	2.963	1×10^{-17}
	umbrella mode	1070	9.346	2×10^{-17}
CH_3OH[d]	OH-stretch	3250	3.077	1×10^{-16}
	CH-stretch	2982	3.354	2×10^{-17}
	CH-stretch	2828	3.536	8×10^{-18}
	CH-deform. \	"1450"	6.897	1×10^{-17}
	and OH-bend /			
	CO-stretch	1026	9.747	2×10^{-17}
$CH_3(CH_2)_4CH_3$[d]	CH-stretch[e]	2955	3.384	1×10^{-17}
		2870	3.484	2×10^{-18}
	CH-stretch[f]	2921	3.424	5×10^{-18}
		2858	3.499	1×10^{-18}
	CH-sciss. \	"1465"	6.826	1×10^{-18}
	and deform.[g] /			
	CH_3-deform.	1370	7.299	2×10^{-19}
CH_3CN[d]	CN-stretch	2270	4.405	2×10^{-18}
$C_4H_8O_2$[d]	C=O stretch	1738	5.754	4×10^{-17}
	CH stretch[e]	2986	3.349	2×10^{-18}
	CH_2 deform.[f]	1450	6.897	8×10^{-18}
	CH_3 deform.[e]	1375	7.273	4×10^{-18}

a) Hagen, Tielens, and Greenberg (1981, 1983); b) Jiang, Person, and Brown (1975); c) Sandford et al. (1988); d) d'Hendecourt and Allamandola (1986); e) per $-CH_3$ group; f) per $-CH_2-$ group; g) per $-CH_3$ and $-CH_2-$.

Note: Integrated absorbance values often depend on neighboring groups and solid-state interactions. See original references for detailed discussion of each absorbance value and range of applicability.

The infrared transmission spectrum through a sample of known thickness is measured when optical constants (n and k) or integrated absorbance values (A) are to be determined. Sample thickness is determined by monitoring the temporal development of the thin film interference pattern of a He-Ne laser beam reflected off or transmitted through the sample during deposition. The infrared spectrum is measured and plotted as log $\{I_o(\nu)/I(\nu)\}$ versus frequency (cm^{-1}), where $I_o(\nu)$ is the single beam spectrum measured through the substrate before sample deposition and $I(\nu)$ the spectrum measured after deposition. For a description of the technique and its application to astrophysics as well as a discussion of how to derive n and k values and A values, see Hagen, Tielens, and Greenberg (1981) and d'Hendecourt and Allamandola (1986), respectively.

One can generally ignore the effects of scattering in the analysis of interstellar infrared absorption spectra because throughout most of the mid-infrared the wavelength is significantly greater than the diameter of the dust grains. In this "Rayleigh limit" the pure absorption term dominates. Scattering becomes important at shorter wavelengths and, under certain conditions, may contribute to the profile of the 3250 cm^{-1} (3.08 μm) H_2O ice band (cf. Allamandola, 1984, and references therein).

III. COMPARISON OF INTERSTELLAR SPECTRA WITH THE SPECTRA OF ICE ANALOGS

In this section interstellar spectra will be directly compared with ice analog spectra. Figure 7 shows one of the earliest direct comparisons of the entire mid-infrared spectrum of an interstellar protostar with the spectrum of a laboratory analog. W33 A is an intense infrared source deeply embedded in a molecular cloud. Estimates of the value of A_v range from 50 to over 100 magnitudes (Capps, Gillett, and Knacke, 1978; Willner et al., 1980). The principle features in both spectra agree reasonably well except in the region around 10 μm where the SiO absorption due to silicates dominates the interstellar spectrum. In the interstellar case, the ice features near 10 μm are presumably so badly blended with the silicate band that they are indiscernable. Carefully measuring the spectral profile of the silicate feature in objects with deep ice bands may reveal some discrepancies with pure silicate profiles (Day, 1979; Knacke and Krätschmer, 1980; Koike et al., 1981). A search for such substructure would be particularly helpful in constraining some of the ice band identifications.

The ice bands will each be discussed in turn, starting with those near 2140 cm^{-1} (4.67 μm). Extensive discussion of the 3250 cm^{-1} (3.10 μm) H_2O band can be found elsewhere (Hagen, Tielens, and Greenberg, 1981; Leger et al., 1983) and it will not be treated further here. We restrict this discussion to the spectroscopic aspects of the comparisons between interstellar and laboratory spectra. See Whittet (1988), for a more general description of the astrophysical implications. A detailed

spectroscopic discussion of many of the bands can be found in Tielens and Allamandola (1987).

The 2500-2000 cm^{-1} (4-5 μm) Region:

Infrared spectroscopy in the 2500-2000 cm^{-1} (4-5 μm) region is a particularly important diagnostic of organic molecules in the interstellar medium because it probes the C≡O, C=C, and C≡N triple-bond

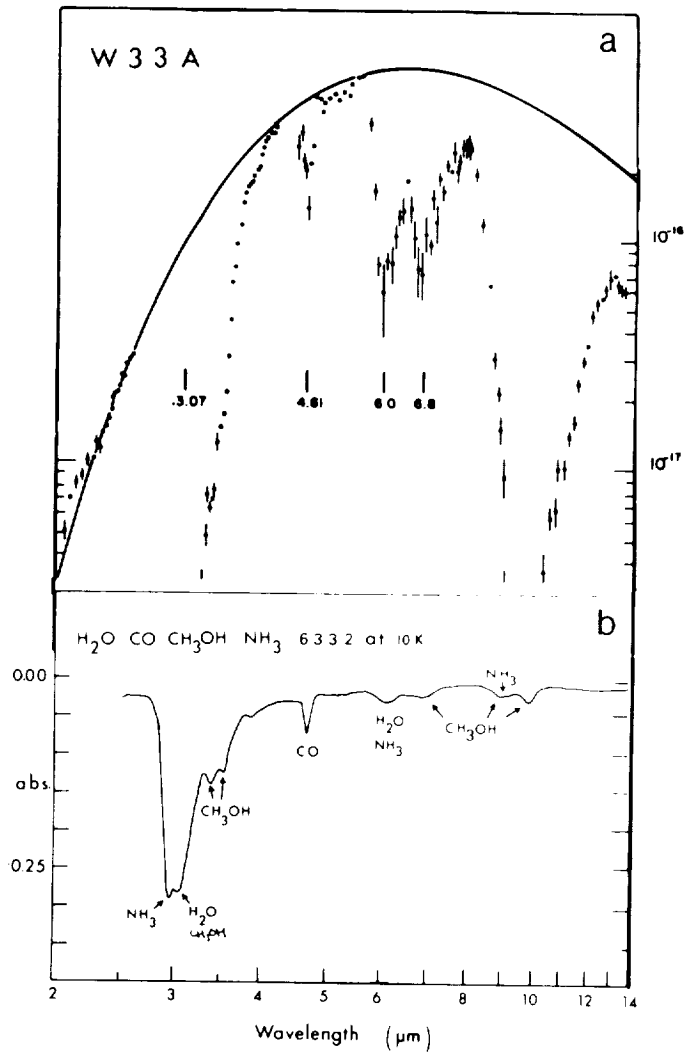

Fig. 7. Comparison of the entire mid-infrared spectrum from W33 A with the spectrum of a laboratory analog. The W33 A spectrum is reproduced from Willner et al. (1980) and the laboratory spectrum from Hagen, Allamandola, and Greenberg (1979).

stretching modes of most molecules (see Figure 3). In interstellar spectra this region is often dominated by a feature near 2138 cm^{-1} (4.667 μm). In several objects there is also an additional band at 2165 cm^{-1} (4.619 μm). The narrow band near 2138 cm^{-1} is due to solid state CO, while the broader feature at 2165 cm^{-1} has been attributed to the CN stretching vibration in an unknown molecule designated X(CN) (Lacy et al., 1984). These two features will be treated separately in the discussion that follows.

Of the 27 objects for which published spectra are available in this region, 16 show a band attributable to frozen CO. The spectral properties of the interstellar solid CO band and derived column densities are listed in Table 2. The width of the interstellar CO band implies that it is present in mixed molecular icy grain mantles (Allamandola, 1984). The position, profile, and cross-section of the CO fundamental for CO in mixed ices depends sensitively on the nature of the ice (Sandford et al., 1988). Figure 8 shows the large spectral variation this band exhibits when the CO is suspended in different solids. The crosshatched areas in the figure indicate the position and full-width-at-half-height (FWHH) of the interstellar CO and X(CN) features. In some sources the CO band seems to consist of a strong, narrow component (5 cm^{-1} FWHH) peaking at about 2140 cm^{-1} (4.673 μm) and a broader component (~ 10 cm^{-1} FWHH) which peaks at about 2135 cm^{-1} (4.684 μm) (Lacy et al., 1984). Comparison of the interstellar spectra with the laboratory spectra shows that the broader 2135 cm^{-1} band in most objects is probably due to CO frozen in an H_2O-rich mantle with an H_2O/CO ratio in the 5-20 range. The narrower band at 2140 cm^{-1} cannot be matched with laboratory spectra of CO intimately mixed with H_2O or any other polar mantle species likely to be important in a molecular cloud. The peak position and width of the narrower band can, however, be matched by CO frozen in a CO_2-rich ice (Sandford et al., 1988). NGC 7538 provides a good example (Figure 9). This is an extremely important result as it provides the first evidence that there are ice mantles which are not dominated by H_2O or other hydrogenated polar species, but rather by non-polar or only slightly polar, non-hydrogenated species. These are precisely the sort of mantles which were predicted to be present in cloud regions where the H/H_2 ratio is substantially less than one (Tielens and Hagen, 1982; d'Hendecourt, Allamandola and Greenberg, 1985).

NGC 7538 is also unique in that the optical depth of the CO feature is exceedingly high. Other objects similar to NGC 7538 may have recently been found. Eiroa and Hodapp (1988), report a source in which the solid state CO band optical depth exceeds that of the 3250 cm^{-1} (3.07 μm) O-H stretch band in H_2O. Preliminary analysis indicates that the CO peak position in this object is also close to 2140 cm^{-1} (4.673 μm), again indicating the dominance of non-polar mantles.

It is important to realize that being able to determine the peak position to an accuracy of about 0.2 cm^{-1} at a frequency of 2140 cm^{-1} implies that an observational resolution of 1 part in 10^4 is required to fully extract the information carried by this band. No other

Table 2. Solid State CO Towards Embedded Objects (from Sandford et al. 1988)

Source Name	Peak Pos. (cm^{-1})	Optical Depth (τ)	FWHM (cm^{-1})	N(CO)-solid $\times 10^{+17}$ (cm^{-2})	Ref.
W33 A					
Narrow	2139.1[d]	0.56	(5)(τ/2)	3.0	a
Broad	2134.8	0.58	(12)(τ/2)	4.4	a
NGC 7538/IRS9					
Narrow	2139.9[d]	2.09	5.0 (τ/2)	11.0	a
Broad	2134.9	0.46	(12)(τ/2)	3.5	a
NGC 7538/IRS1	2139.9[d]	0.24	3.5 (τ/2)	0.76	a
W3/IRS 5	2140[d]	0.20	4.6 (τ/2)	0.83	a
Elias 1	2135±2	0.10	~10-20 (τ/2)	0.9	b
Elias 7	2135±2	0.13	~12 (τ/2)	0.9	b
Elias 13	2136±2	0.22	~10 (τ/2)	1.3	b
Elias 16	2141±2[d]	0.96	~5 (τ/2)	4.5	b
Elias 18	2140±2[e]	0.35	~11 (τ/2)	2.9	b
GL 2136	2137±2	0.15	~7	0.62	c
OMC-2/IRS3	2137±2	0.10	~10	0.59	c
GL 490	2140±2	0.15	~5	0.68	c
NGC 2024/IRS2	2137±2	0.35	7	1.4	c
GL 961	2137±2	0.30	11	1.9	c
GL 989	2137±2	0.35	9	1.9	c
Mon R2/IRS2	2137±2	0.30	9	1.6	c

a) Lacy et al. (1984)
b) Whittet, Longmore, and McFadzean (1985)
c) Geballe (1986)
d) For these features, A = 1.0×10^{-17} cm/molecule for pure CO was used rather than A = 1.7×10^{-17} cm/molecule, the value for CO in water ice.
e) The profile of this feature indicate that it is comprised of comparable amounts of the broad and narrow solid CO bands. N(CO) was determined by arbitrarily assuming that half the band area was due to the narrow component and half to the broad component.

interstellar ice feature we are presently aware of requires such resolution for analysis. In most cases 1 part in 10^3 is sufficient. The unique combination of the ability to measure the interstellar CO feature with such precision, in conjunction with the high sensitivity of the solid state CO band position and profile to the nature of the solid, provides far more insight into the nature of the cloud (solid state properties as well as gas phase chemistry) than even the most optimistic analog afficionados anticipated a few years ago.

While the observed CO band profiles can be explained by simple accretion and grain surface chemistry, the X(CN) band at 2165 cm^{-1} (4.619 μm) indicates that processing by radiation also occurs. Laboratory studies carried out by van de Bult in 1982 and 1983 (Leiden University, unpublished results) showed conclusively that the 2165 cm^{-1} feature could be produced in ices comprised of species expected on the basis of accretion only if they were irradiated and if they contain

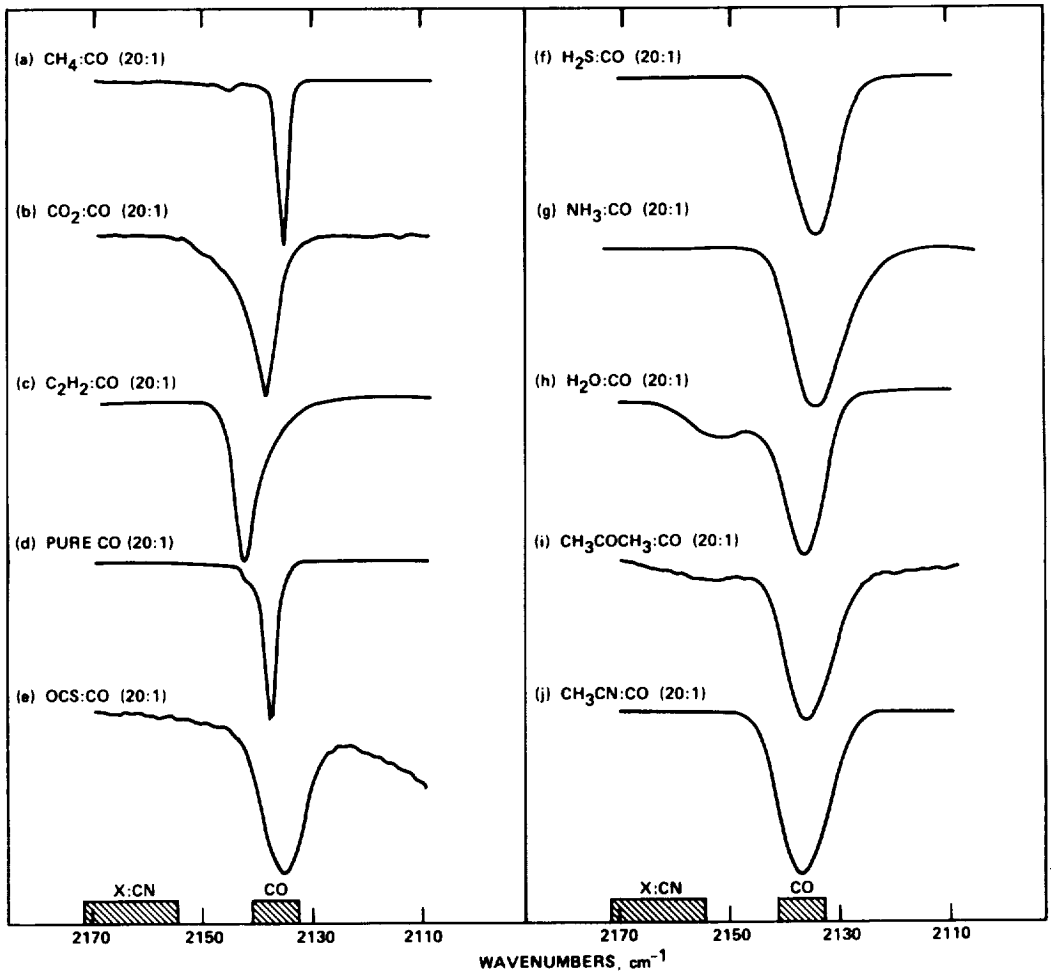

Fig. 8. The CO absorption band for CO suspended in various ices at 10 K. Figure adapted from Sandford et al. (1988).

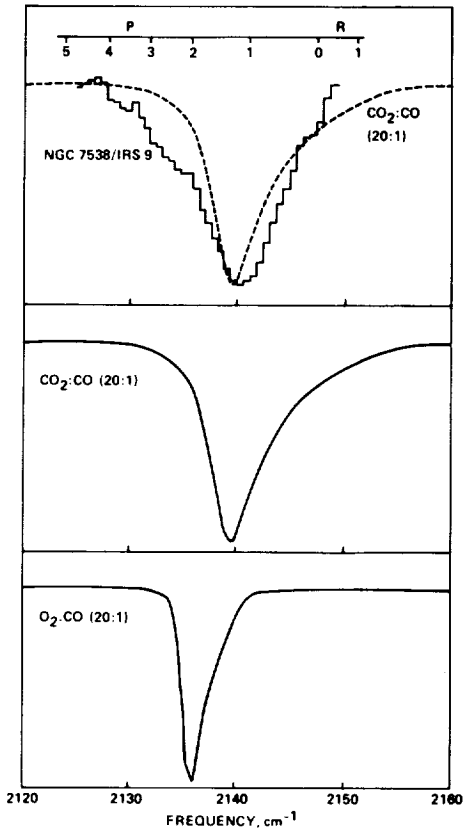

Fig. 9. The solid CO absorption feature in NGC 7538/IRS 9 compared to the bands produced when CO is suspended in solid CO_2 (middle) and O_2 (bottom) at 10 K. Figure adapted from Sandford et al. (1988)

sources of C and N atoms which can be freed from their parent species by energetic processes. Several of these experiments are described in Lacy et al. (1984). Further photochemical studies regarding this band are described in d'Hendecourt et al. (1986) and Grim and Greenberg (1987). This band is also produced in ices bombarded by ions (Moore et al., 1983). Figure 10 shows a comparison of the spectrum of W33 A with the laboratory spectrum of an irradiated ice which had been warmed to eliminate most of the more volatile CO. The X(CN) feature at 2165 cm^{-1} provides a good fit to the astronomical data and was originally thought to be due to a nitrile or isonitrile. Recently, however, it has also been suggested that the band is produced by the CN stretch of the OCN^- ion (Grim and Greenberg, 1987). The ion assignment must be tested further in the laboratory. Until it is, the exact identification of this band remains somewhat uncertain. In any event, it appears that the source of the interstellar 2165 cm^{-1} band contains a CN bond and is produced by the energetic processing of pre-existing ice mantles.

In addition to the 2140 and 2165 cm^{-1} features, the spectrum of W33 A also shows two weak bands at 2525 and 2043 cm^{-1} (3.960 and 4.895 μm) which are thought to be associated with the ice mantles (Geballe et al., 1985; Larson et al., 1985). The former band has been attributed to H_2S. Candidates proposed for the identification of the latter band include a sulfur-containing compound like OCS (Geballe et al., 1985), methanol (CH_3OH), and the radicals C_3 and CN (Larson et al., 1985).

The 2000-1250 cm^{-1} (5-8 μm) Region:

Infrared spectroscopy in the 2000-1250 cm^{-1} (5-8 μm) region is important because it probes the C-H, N-H, and O-H bending and deformation modes as well as the C=O, C=C, and C=N double-bond stretching modes of most molecules. It is the only part of the spectrum where the types of molecule which contain carbonyl groups (C=O) can be

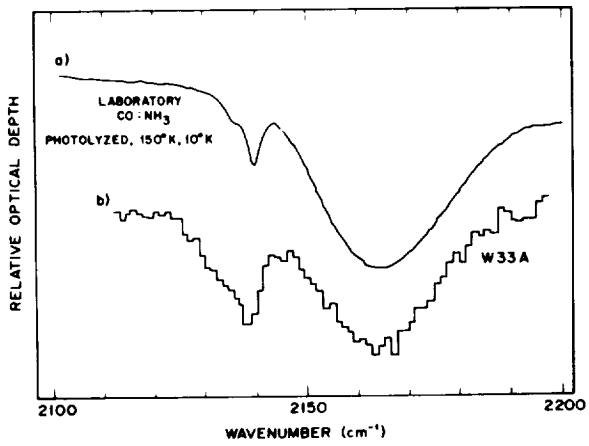

Fig. 10. The laboratory spectrum in the 2100-2200 cm^{-1} (4.5-4.8 μm) region of an NH_3/CO ice which has been photolyzed and warmed up to 150 K compared to the spectrum of W 33A. Figure adapted from Lacy et al. (1984).

classified. The importance of this spectral region is amplified in the interstellar case because strong, broad absorption features in the 3 and 10 μm regions, due to the O-H stretch in H_2O and the Si-O stretch in silicates, respectively, considerably hamper the detection of other absorption features. The discussion in this section relies heavily on the previous review by Tielens and Allamandola (1987).

Figure 11 shows a number of 2000-1250 cm^{-1} (5-8 μm) spectra of embedded protostars taken using the Kuiper Airborne Observatory (Tielens and Allamandola, 1987; Tielens et al., 1988). All the spectra show prominent absorption features peaking around 1670 and 1460 cm^{-1} (5.99 and 6.85 μm). The signal-to-noise in these spectra is sufficiently high to permit a comparison of the profiles and substructures of these features. They show a continuous variation from relatively narrow bands like those in W33 A to much broader ones. The apparent increase in the width of some of the bands is caused by the increasing importance of additional absorption features near 1720, 1500, and 1410 cm^{-1} (5.81, 6.67, and 7.09 μm). The 1670 and 1460 cm^{-1} features are treated separately in the discussion that follows.

The 1670 cm^{-1} (5.99 μm) band is generally attributed to the H-O-H bending mode of H_2O. In fact, the relatively narrow feature in W33 A (as well as in NGC 7538-IRS 9 and AFGL 2136) can be well matched by simple H_2O ice spectra (Figure 12a). The objects with a wider 1670 cm^{-1} feature require that additional components be present, however. The short wavelength wing on the 1670 cm^{-1} feature, which is not prominent in the W33 A spectrum, is attributed to absorption by the C=O stretching mode in carbonyl-bearing molecules. Possible identifications include ketones like acetone (CH_3COCH_3) and aldehydes like formaldehyde (H_2CO). The presence of formaldehyde is supported by the suggestion of substructure at 1500 and 1410 cm^{-1} (6.67 and 7.09 μm) in some of the spectra. Higher resolution studies are needed to verify the presence of these features.

It has also been suggested that the 1670 cm^{-1} (5.99 μm) feature could be due to the H-O-H bending mode of H_2O molecules adsorbed or

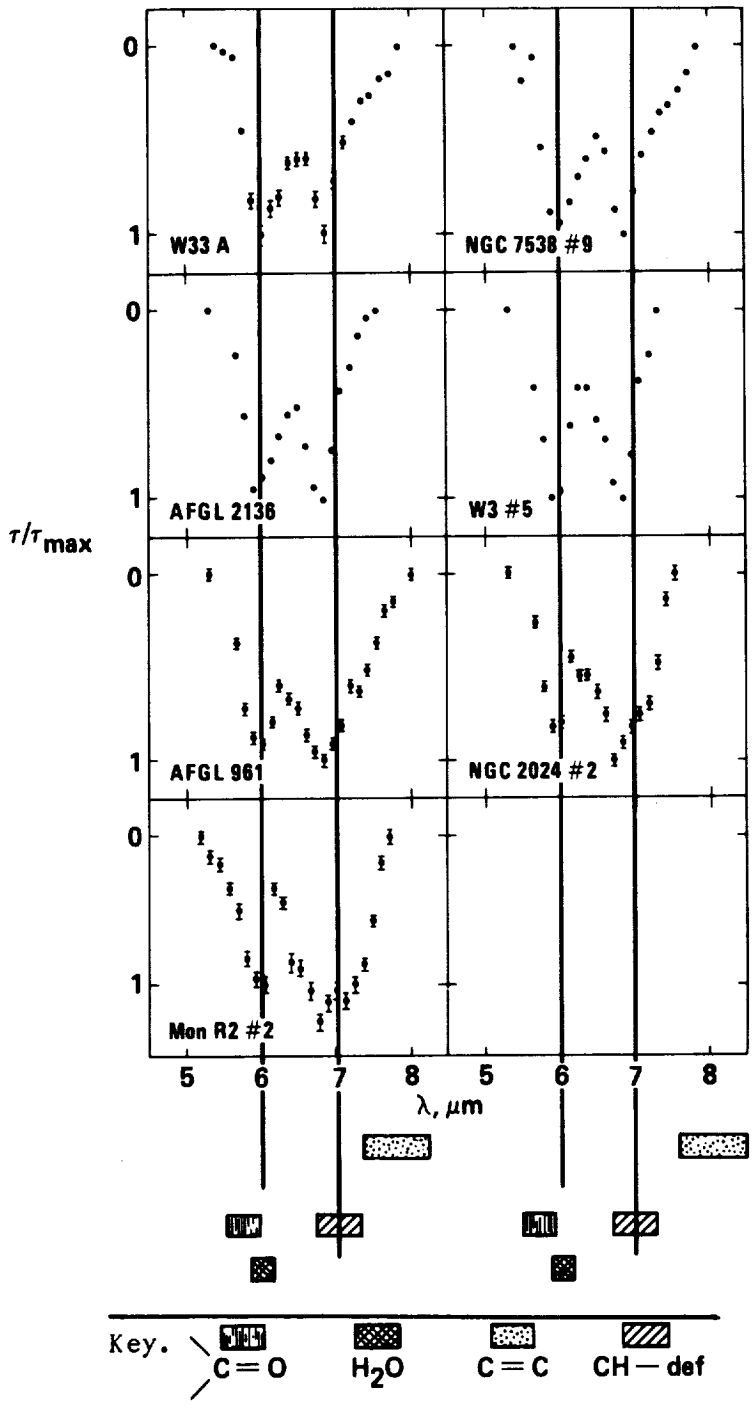

Fig. 11. The 2000-1250 cm^{-1} (5-8 μm) spectra of several protostars obtained with the Kuiper Airborne Observatory. Spectra taken from Tielens et al. (1988). The spectral ranges indicated by the various shaded boxes below the figure indicate the vibrational frequency regions appropriate for each molecular subgroup.

absorbed in hydrated or layer-lattice silicates (Knacke and Krätschmer, 1980; Sandford and Walker, 1985; Hecht et al., 1986). For example, strong "hydration" bands are seen in the spectra of many interplanetary dust particles (Sandford and Walker, 1985) which are known to contain interstellar components (McKeegan et al. 1985). However, the O-H deformation modes in such materials usually peak between 1640 and 1600 cm^{-1} (6.09 and 6.25 μm), i.e. at too low a frequency to match the deepest part of the interstellar feature, and they produce bands that are too narrow. These materials, however, may contribute to the long wavelength wing seen in many of the 1670 cm^{-1} features. Thus, although hydrated silicates may well be present, it appears that they are not the dominant source of the interstellar 1670 cm^{-1} feature.

The major feature at 1460 cm^{-1} (6.85 μm) has been the recipient of a number of identifications. At present, this band is generally attributed to the C-H deformation mode in simple alcohols like methanol (CH_3OH) (Tielens and Allamandola, 1987; Tielens et al., 1988). The laboratory spectra of these molecules agree quite well with the feature in W33 A and NGC 7538 (Figure 12a). Figure 12b provides an illustration that the C-H deformation modes of pure hydrocarbons (in this case hexane, C_6H_{14}) do not provide a satisfactory match to the interstellar feature. The position of the C-H deformation mode in methyl ($-CH_3$) and methylene ($-CH_2-$) groups depends on the species to which they are attached, an effect illustrated in Figure 13. Thus, the change in the peak position and profile of the "1470" cm^{-1} band shown in Figure 11 indicates a wide variation in the relative importance of different types of hydrocarbons from one cloud to another.

Another identification of the 1460 cm^{-1} (6.85 μm) feature has also been suggested. Knacke and Krätschmer (1980) and Sandford and Walker

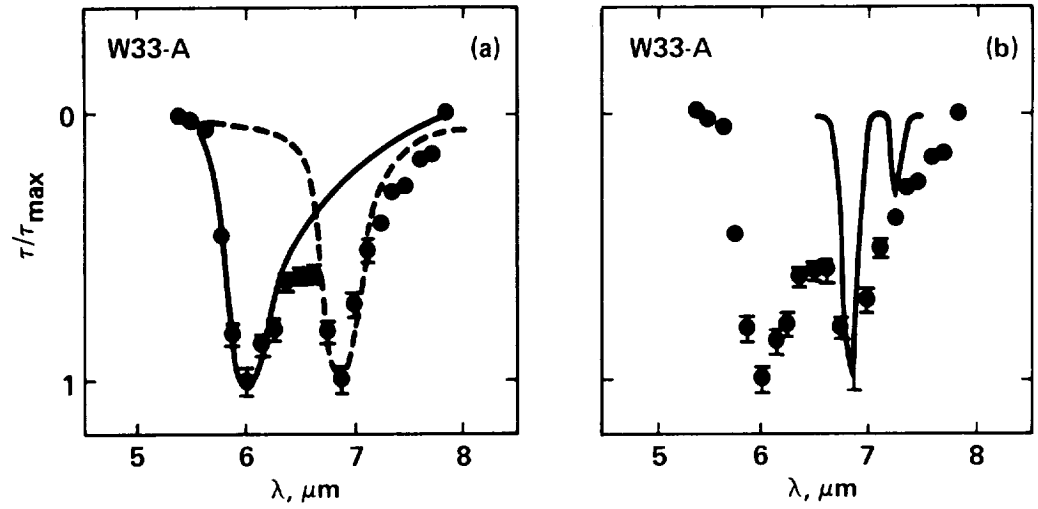

Fig. 12. Comparison between the 2000-1250 cm^{-1} (5-8 μm) spectrum of W33 A (dots) with (a) the laboratory spectrum of H_2O (solid line) and CH_3OH (dashed line) ices at 10 K, and with (b) the laboratory spectrum of C_6H_{14} (solid line).

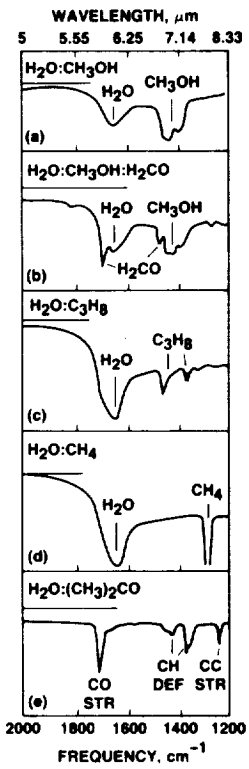

Fig. 13. Laboratory spectra of several H_2O-rich ices containing different hydrocarbons illustrating that the C-H deformation falls at different frequencies in the 1500-2000 cm^{-1} (6.6-8.3μm) region.

(1985) have suggested that the asymmetric stretch of the CO_3 anion in carbonates may be responsible for some of this feature. This possibility is worth considering since carbonates are known to exist in many interplanetary dust particles (Sandford, 1986; Tomeoka and Buseck, 1986). Many of these same particles contain isotopic anomalies, demonstrating that at least some of their material has an interstellar origin (McKeegan et al., 1985). The feature produced by carbonates in IDPs provides a good match to that seen in the W33 A spectra. However, while carbonates can provide a broad feature in the correct region of the spectrum, they cannot easily reproduce the details of the subfeatures and profile variations seen in the more complex astronomical spectra (cf. NGC 2024#2 in Figure 11). Thus, we are led to conclude that, while other components may well be present, ices are largely responsible for the 1460 cm^{-1} feature.

There are also two weak features in the spectrum of NGC 7538-IRS 9, a relatively narrow one (FWHH ≈ 35 cm^{-1}) at 1820 cm^{-1} (5.49 μm) and a much broader one (FWHH ≈ 85 cm^{-1}) at about 1310 cm^{-1} (7.63 μm). The presence of the 1310 cm^{-1} feature in NGC 7538 has been confirmed by a higher resolution study (Tielens et al., 1988). This band is also present in the spectrum of W33 A. The 1820 cm^{-1} feature is attributed to the C=O stretch in organic peroxides or carbonyl-containing radicals like HCO or HOCO. The 1310 cm^{-1} (7.63 μm) feature may be the absorption counterpart of the 1300 cm^{-1} (7.7 μm) emission feature, attributed to polycyclic aromatic hydrocarbons (PAHs) and related materials. This feature can be used to set an upper limit on the amount of PAHs and amorphous carbon absorbing along the lines of sight to these sources. In clouds, a significant fraction of the PAH population is expected to be frozen in grain mantles. High resolution searches for absorption by the 1610 cm^{-1} (6.21 μm) aromatic CC stretch feature is very important to test this identification in these sources.

Thus, while the absorption in the 2000-1250 cm^{-1} (5-8 μm) spectral region probably contains contributions from a wide variety of materials,

it appears that ices are responsible for the majority of the absorption. Certainly a reasonably good fit to most of the interstellar absorption features can be obtained using only icy materials. While it may seem a bit premature to consider some band carriers as identified and attempt to quantify their relative abundances and column densities, it is nonetheless a useful exercise since the admittedly tentative results can provide important insights into the nature of dust in dense clouds and establish a framework on which to base future work. It is in this spirit that Table 3 is presented, assuming only icy materials are present. Table 3 contains estimates of the relative amounts of the various interstellar ice components in different clouds. The reader should see Tielens and Allamandola (1987) for a detailed discussion of the limitations and assumptions that went into producing this table. In considering this listing, bear in mind that the data on which these values are based are obtained by viewing through a cloud, and projection effects are important. For example, the presence of much more CO frozen in non-polar ices (possibly CO_2) than in H_2O-rich ices in NGC 7538 (Sandford et al., 1988) and perhaps in the Serpens cloud (Eiroa and Hodapp, 1988) seems to indicate that the H/H_2 ratio can vary substantially from one cloud to another. At present there is no way to determine the relative importance of polar versus non-polar ices in clouds apart from the CO band. In this respect, high resolution spaceborne studies of CO_2 (and perhaps O_3, as this is the other major non-polar mantle constituent predicted by the models) in interstellar ices should prove very informative.

It is difficult to understand how the processes which led to the relatively simple 2000-1250 cm^{-1} (5-8 μm) spectra exhibited by W33 A and NGC 7538-IRS 9 could be modified by changing only cloud density and opacity and produce the variations in band breadth and substructure shown by the other sources. Thus the richness of compositional variation implied by the differences in the interstellar spectra suggests that energetic processing of the ices is the rule rather than the exception.

IV. PHOTOCHEMICAL AND THERMAL EVOLUTION OF INTERSTELLAR AND PRE-COMETARY ICE ANALOGS

Infrared spectra of several energetically processed ices are now available for comparison with the astrophysical data. To date most studies have focused on polar ices (Hagen, Allamandola, and Greenberg, 1979; Moore et al., 1983; Strazzulla et al., 1984; Strazzulla, 1985; Agarwal et al., 1985; Allamandola, Sandford, and Valero, 1988; Khare et al. 1988; Schutte, 1988), while only a few studies have included non-polar, mixed molecular ices (Strazzulla et al., 1984; d'Hendecourt et al., 1986). In general, most of the carbon in these experiments has been provided by CH_4. In view of the arguments in favor of CH_3OH in interstellar ices, it is important to carry out a similarly thorough experimental program on ices containing this molecule. In particular, it will be interesting to find out if the relative amounts of the various products formed by high energy particle bombardment differ

Table 3. Composition of Interstellar Grain Mantles[a,b]

Species	W3 IRS 5	NGC2024 IRS2[c]	MonR2 IRS2[c]	AFGL 961	W33 A	AFGL 2136	NGC7538 IRS9
H_2O	1.	1.	1.	1.	1.	1.	1.
CH_3OH[d]	0.81	1.75	3.0	0.87	0.55	0.66	0.65
CO	0.05	0.22	0.20	0.06	0.02	0.04	0.16
Carbonyl	0.05	0.15	0.64	0.04	--	0.04	0.01[e]
Aldehyde	0.05	0.35	0.55	0.13	--	--	--
Ketones	--	0.65	1.3	0.21	--	--	--
CH_4	--	--	0.05	0.015	0.005	--	0.01
NH_3	<0.10	--	--	0.10	0.10	0.10	0.10

a) Taken from Tielens and Allamandola (1987)
b) All abundances normalized to H_2O
c) H_2O and CH_3OH abundance not well determined [see Tielens et al. (1988)]
d) Abundance of CH_2 and CH_3 groups based on the A value of the combination C-H deformation and O-H bending modes in methanol
e) Determined from the 1820 cm^{-1} (5.49 μm) feature

significantly from those produced by ultraviolet irradiation. A difference might be expected since CH_3OH is very sensitive to ultraviolet radiation (it dissociates upon absorption of photons out to wavelengths of about 2000 Å, in contrast to species like H_2O and CH_4 which have photo-dissociation thresholds that require shorter wavelength radiation), whereas high energy particles deposit sufficient energy for dissociation in a non-selective manner.

We present the following example as an illustration of the processes which occur upon ultraviolet irradiation of CH_3OH containing ices. A more detailed discussion of these experiments and the astrophysical implications can be found elsewhere (Allamandola, Sandford, and Valero, 1988).

$H_2O:CH_3OH:NH_3:CO$ (100:50:1:1)

Figure 14 shows the spectral development of a long duration photolysis of an $H_2O:CH_3OH:NH_3:CO$ (100:50:1:1) ice mixture. Infrared spectra were taken after 1, 9, and 37 hours of irradiation. The photochemical evolution of this mixture is shown graphically in Figure 15 where the abundance of each molecule is plotted versus photolysis time. Inspection of Figures 14 and 15 show that H_2CO, CH_4, CO_2, and HCO are produced, largely at the expense of CH_3OH. Very long irradiation (37 hours) destroyed nearly all the CH_3OH and it appears that some of the H_2CO produced during the early irradiation stage (10 hours) was photo-oxidized to CO and CO_2. The later oxidation of H_2CO is probably due to reduced screening of ultraviolet photons by CH_3OH which absorbs more strongly across the ultraviolet than does H_2CO (Calvert and Pitts 1966). Blending of the C-H stretching bands in the 3000-2900 cm^{-1} (3.3-3.4 μm) region with the O-H stretching band produces a false continuum which leads to underestimates of the abundances of hydrocarbons present if this region alone is analyzed.

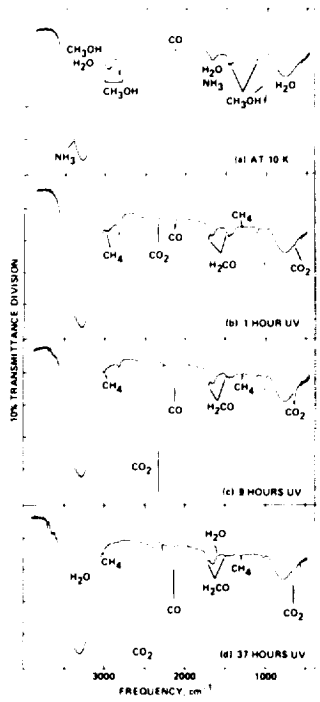

Fig. 14. The infrared spectra of an $H_2O:CH_3OH:NH_3:CO$ (100:50:1:1) ice taken at 10 K (a) before and after (b) 1, (c) 9, and (d), 37 hours of ultraviolet photolysis.

A similar mixture ($H_2O:CH_3OH:NH_3:CO$ = 100:50:10:10) was also deposited and irradiated in order to study the low volatility material produced by photolysis. Figure 16 shows the spectra (each taken at 10 K) of this residual material after the substrate was temporarily warmed to 200, 250, and 300 K under vacuum. The figure shows that, while the bulk of the low volatility material produced by photolysis leaves between 250 and 300 K, some remains at 300 K.

$H_2O:CH_3OH:NH_3:CO:C_3H_8$ (100:50:10:10:10)

Figures 17 and 18 present spectra of an $H_2O:CH_3OH,NH_3:CO:C_3H_8$ (100:50:10:10:10) ice sample taken at 10 K and after 1, 6, 9, and 15 hours of ultraviolet photolysis followed by warm-ups to30, 55, and 100 K. The photochemical evolution of molecular abundances in this sample is shown graphically in Figure 19. This and the following experiment were done to determine how the nature of a hydrocarbon initially present in the ice affects the character of the hydrocarbons in the resulting resi-

dues. The major difference between the spectra in Figures 14a and 17a is the addition in the latter of the C-H stretch and deformation bands of C_3H_8 ($H_3C-CH_2-CH_3$) in the 2900-2800 and 1500-1400 cm^{-1} regions, respectively. The photochemical behavior of this mixture is similar to that in the previous experiment in that H_2CO, CH_4, CO_2, CO, and HCO are produced, while CH_3OH is destroyed. The spectrum taken after 9 hours of irradiation (Figure 17d) is very similar to the 9 hour irradiation spectrum of the $H_2O:CH_3OH:NH_3:CO$ (100:50:1:1) ice shown in Figure 14c. The major difference between these two 9 hour irradiation spectra is that bands due to unconsumed C_3H_8 and weak X(CN) and residue bands (at 2160 and 1580 cm^{-1}, respectively), are only present in Figure 17d. Note again the blending of the C-H stretch bands in the 3000-2900 cm^{-1} region with the strong O-H band.

The spectra shown in Figure 18 illustrate several interesting points. Between 10 and 30 K the spectra are virtually unchanged, indicating that the volatile species CO and CH_4 are tightly trapped in the ice. Between 30 and 55 K the bands due to both CO and CH_4 diminish while the rest of the spectrum remains unchanged. This occurs because

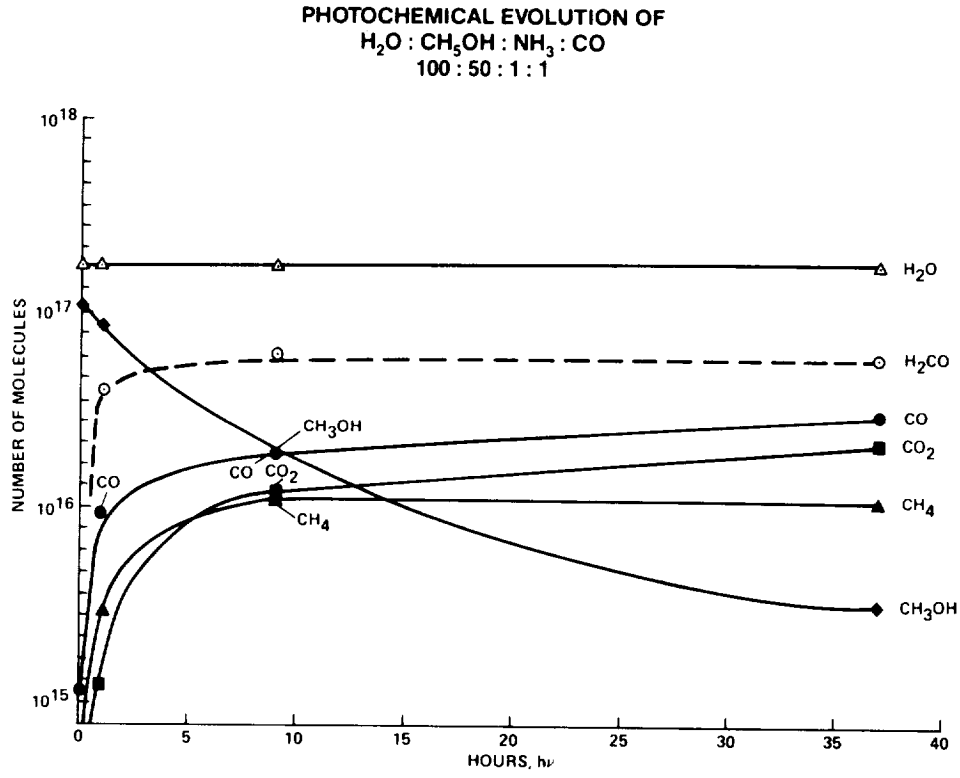

Figure 15. The abundance of parent and product molecules in the $H_2O:CH_3OH:NH_3:CO$ (100:50:1:1) sample as a function of photolysis time. The H_2CO abundance is given as a dashed line since its A value in H_2O-rich ices is only estimated. The ultraviolet photon flux striking the sample area is about $5x10^{17}$ hr^{-1}.

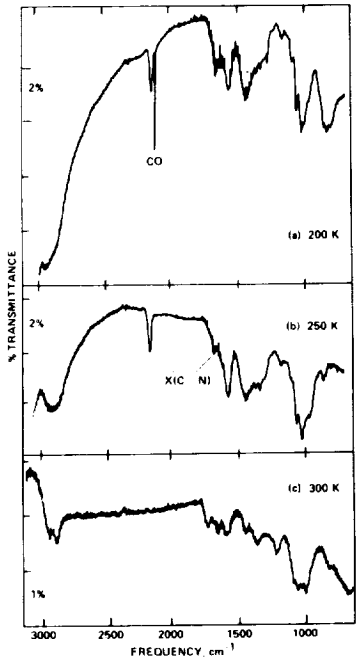

Fig. 16. The infrared spectra (taken at 10 K) of the low vapor pressure materials produced by the 9 hour photolysis of an H_2O:CH_3OH:NH_3:CO (100:50:10:10) ice after temporary warm-up to (a) 200, (b) 250, and (c) 300 K.

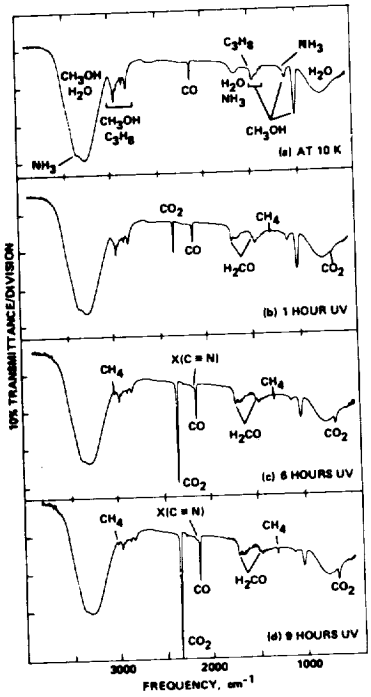

Fig. 17. The infrared spectra of an H_2O:CH_3OH:NH_3:CO:C_3H_8 (100:50:10:10:10) ice taken at 10 K (a) before and after (b) 1, (c) 6 and (d) 9 hours of photolysis.

CO and CH_4 can migrate slowly through the ice in this temperature range and can escape (see Sandford and Allamandola 1988 for a discussion of CO loss from H_2O ice). At 100 K, only 25% of the CO and 28% of the CH_4 initially present just before warm-up remains. The profile of the 3275 cm^{-1} H_2O band becomes asymmetric and narrower in the 100 K spectrum, indicating that the solid H_2O is transforming from the amorphous to cubic form. Apart from CH_4, there is no other loss of hydrocarbons up to 100 K.

Warm-up to 200 K was sufficient to remove most of the parent molecules from the sample, leaving a mixture comprised primarily of low volatility photoproducts. Spectra of these materials taken at 10 K after temporary warm-up to 200, 250, and 300 K are shown in Figure 20. The bulk of the residue sublimes away between 200 and 250 K. The

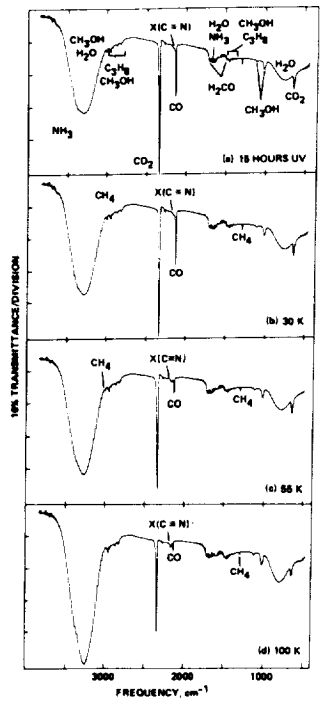

Fig. 18 The infrared spectra of an H_2O:CH_3OH:NH_3:CO:C_3H_8 (100:50:10:10:10) ice irradiated for 15 hours taken at 10 K (a) after temporary warm-up to (b) 30, (c) 55 and (d) 100 K.

spectral evolution in the C-H stretching region from 3100-2600 cm^{-1} is presented on an expanded scale in Figure 21. The C-H stretching band profile indicates that the residue contains both methyl ($-CH_3$) and methylene ($-CH_2-$) groups. Figure 21 shows that there are at least two components in the residue. The first is principally responsible for the $-CH_3$ stretching bands at about 2960 and 2870 cm^{-1} which largely disappear by 250 K, behavior similar to that of the C≡N band at 2158 cm^{-1} (Figure 20). There are at least two $-CH_2-$ components, one giving rise to the bands at about 2925 and 2850 cm^{-1}, and the other producing bands at about 2910 and 2840 cm^{-1}. The first pair is largely gone by 250 K and thus may be related to the $-CH_3$, and possibly the C≡N, carrier. The second $-CH_2-$ carrier remains to 300 K. The band profile and position of the 300 K fraction is quite similar to that of the residue produced in the previous experiment in which CH_3OH was the only hydrocarbon present in the initial ice. The relative intensities of the $-CH_3$ and $-CH_2-$ bands in the 300 K spectra indicate that $-CH_2-$ groups dominate the structure of this fraction of the residue. This implies long hydrocarbon chains are responsible. A chain structure is consistent with the observed low volatility of this material and represents a significant change from the $-CH_3$ dominated parent molecules, C_3H_8 ($H_3C-CH_2-CH_3$), and CH_3OH.

Additional experiments, where the C_3H_8 was replaced by C_6H_{14} (hexane), yielded similar results. The strong similarity between the residue spectra and warm-up behavior of these two experiments indicates that the $-CH_3/-CH_2-$ ratio of the complex molecules formed by photolysis does not depend strongly on the $-CH_3/-CH_2-$ ratio of the parent hydrocarbon in the ice prior to photolysis (Allamandola, Sandford and Valero, 1988).

V. THE NATURE OF THE COMPLEX MOLECULES PRODUCED BY PHOTOLYSIS AND ASTROPHYSICAL IMPLICATIONS.

The richness of the 200 K spectra shown in Figures 16 and 20, and the changes in relative band strengths which occur upon warm-up from 200 to 300 K, indicate that species of varying complexity have been produced. Apart from being important in the chemical evolution in the

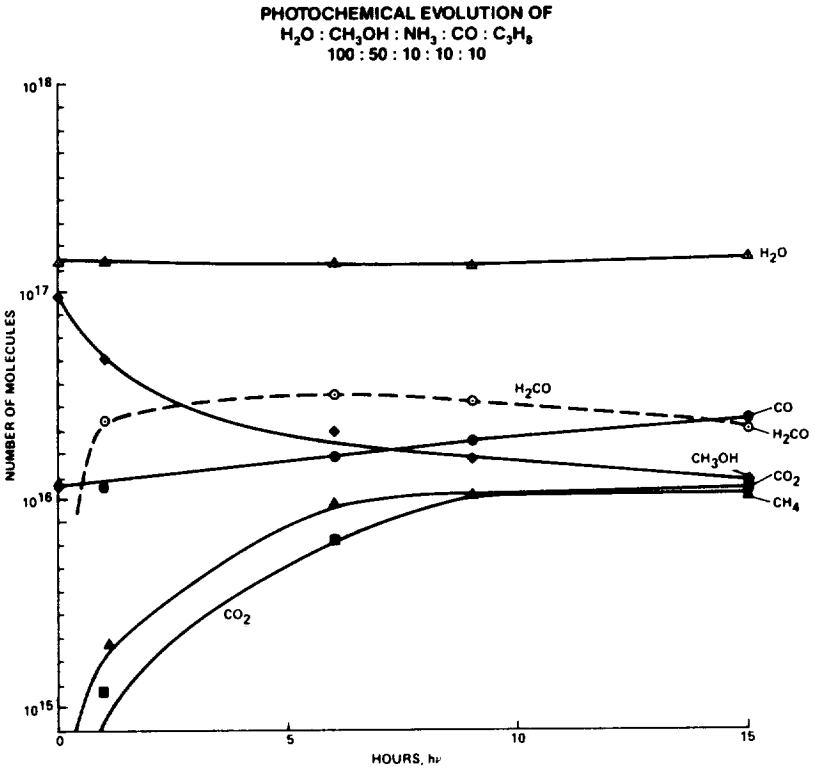

Fig. 19. The abundance of parent and product molecules in the H_2O:CH_3OH:NH_3:CO:C_3H_8 (100:50:10:10:10) sample as a function of photolysis time. The H_2CO abundance is given as a dashed line since its A value in H_2O-rich ices is only estimated. The ultraviolet photon flux striking the area sampled by the infrared spectrometer is about 5×10^{17} hr^{-1}.

interstellar medium, these results have applications to solar system processes as well. For example, the observed differential sublimination of these moderately volatile compounds may regulate the scale heights of some of the molecular photo-fragments seen in cometary comae (Delsemme and Miller, 1971).

All the 200 K spectra have a prominent band at 1580 cm^{-1}. This band and the one at 2168 cm^{-1} are the only "residue" features evident before warm-up. The 2168 cm^{-1} band, which we identify with a nitrile or iso-nitrile (-C≡N or C≡N-) bearing compound, leaves between 200 and 250 K, suggesting that it is part of a small molecular species. These molecules may be similar to those ejected in ice particles, freed by sublimation, and processed by solar photons to produce the C≡N jets observed in Comet Halley (A'Hearn et al., 1986).

The presence of several different types of $-CH_3$ and $-CH_2-$ bearing molecules in the residues is shown by the spectral structure in the 3000-2700 cm^{-1} region in Figure 21. As just pointed out, the similar

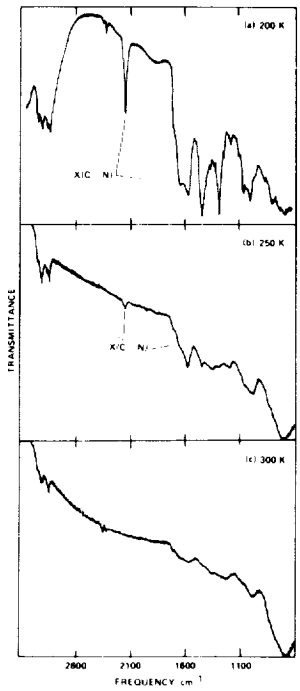

Fig. 20. The infrared spectra taken at 10 K) of the low vapor pressure materials produced by the 15 hour photolysis of an H_2O:CH_3OH:NH_3:CO:C_3H_8 (100:50:10:10:10) ice after temporary warm-up to (a) 200, (b) 250, and (c) 300 K.

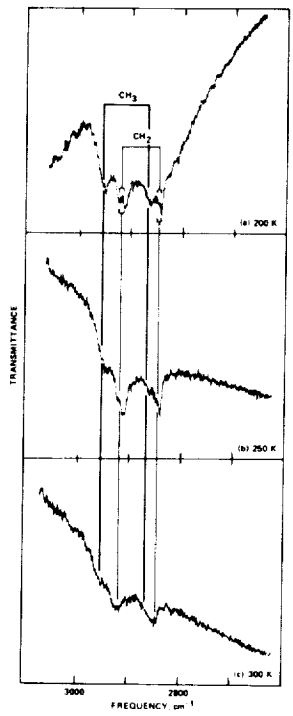

Fig. 21. The infrared spectra (taken at 10 K) in the C-H stretch region of the low vapor pressure materials produced by the 15 hour photolysis of an H_2O:CH_3OH:NH_3:CO:C_3H_8 (100:50:10:10:10) ice. The data are identical to those in Figure 20, but are plotted on an expanded scale to demonstrate the behavior of the various hydrocarbon components upon warm-up.

evaporation behavior of some of the bands indicates that they may be related. In particular, the simultaneous loss of the bands assigned to C≡N, $-CH_3$, C=O, and one of the $-CH_2-$ components suggests the possibility of a common carrier.

The spectra of the residues remaining at 300 K show that they are $-CH_2-$ rich, independent of the $-CH_2-/-CH_3$ ratio in the original ice. The relatively non-volatile behavior of this component is consistent with the molecular structures implied. Because methyl ($-CH_3$) groups are chain terminating, while methylene ($-CH_2-$) groups are chain lengthening, $-CH_3$ rich compounds either consist of shorter hydrocarbon chains or are

highly branched, while $-CH_2-$ rich compounds contain longer hydrocarbon chains. Chain-like structures interact more strongly with their environment than do more compact structures. Consequently, all other interactions being equal, $-CH_2-$ rich hydrocarbons have lower vapor pressures than $-CH_3$ rich hydrocarbons.

The peak position and profile of the C-H stretching feature in the spectrum of dust toward the galactic center shows that it is $-CH_2-$ rich (Allen and Wickramasinghe, 1981; Jones et al., 1983). The grains along this line-of-sight are thought to be representative of interstellar dust in diffuse, highly photo-processed regions. The observation of a $-CH_2-$ rich hydrocarbon is therefore consistent with a non-volatile, complex material in the diffuse interstellar medium. This is similar to the aliphatic hydrocarbon component found in interplanetary dust particles (Swan et al., 1987).

In contrast, the profile and peak position of the emission feature near 2990 cm^{-1} (3.34 μm) observed in the spectra of Comets Halley and Wilson imply that the cometary carrier(s) are dominated by $-CH_3$ groups (Wichramasinghe and Allen, 1986; Tokunaga et al., 1986; Baas, Geballe, and Walther, 1986; Danks et al., 1987; Knacke, Brooke, and Joyce, 1986). Our most refractory material provides a better match to the interstellar spectra than the cometary spectra. The apparent mismatch between our 300 K residue spectra and the cometary data suggests that either (i) the $-CH_3$ rich material that leaves between 200 and 300 K is more representative of the cometary materials responsible for the emission, or (ii) that our original samples lack an important component.

The peak position of the observed cometary feature falls at the high frequency extreme of the normal spectral range for saturated aliphatic hydrocarbons, implying that the $-CH_2-$ and $-CH_3$ groups are attached to strongly electronegative moieties. The recent proposal that polycyclic aromatic hydrocarbons (PAHs) and related materials are ubiquitous and abundant in space (Duley and Williams, 1981; Leger and Puget, 1984; Allamandola, Tielens, and Barker, 1985) suggests that PAHs may be a component of interstellar and cometary ices. PAHs, which are very electronegative, could be present with abundances as high as about 10% that of H_2O and still not be detectable in protostellar absorption spectra since these molecules are poor absorbers in the infrared. In fact, there is a broad, weak absorption centered near 1300 cm^{-1} in the spectra of the protostellar objects W33A and NGC 7538 which is consistent with PAHs or amorphous carbon (see Section III and Tielens and Allamandola, 1987). Certainly aromatic moieties are present in the carbonaceous components of primitive meteorites and interplanetary dust particles (Hayatsu and Anders, 1981; Allamandola, Sandford, and Wopenka, 1987), both of which may have a cometary origin.

Finally, it is interesting to consider these results in light of the recent suggestion that polyoxymethylene (POM), a polymer of formaldehyde $[-(CH_2-O)_n-]$, may exist in comets (Huebner, Boice, and Sharp, 1987). The work reported here, as well as that of others, shows that H_2CO is readily produced during the irradiation of ice analogs.

Irradiation of H_2CO-rich residues might well produce some POM. However, the observed differential evaporation implies that the residue material is not dominated by a simple repeating structure like that of POM.

VI. CONCLUSIONS

Infrared absorption spectra of dense molecular clouds, when compared with laboratory spectra of interstellar ice analogs, provide a powerful means of probing the chemical composition of interstellar, precometary dust and the physical and chemical nature of the various environments in which it is found. This comparison indicates that the bulk of the interstellar absorption features are due to mixed molecular ices containing many organic molecules.

The 2138 cm^{-1} (4.677 μm) band is due to solid CO. Analysis of the different profiles and positions of this feature provides strong evidence that clouds contain two distinct types of ice: one characterized by polar, hydrogen-bonding molecules like H_2O, and the other characterized by non-polar, or only slightly polar, species such as CO_2. The first type of ice is thought to be produced in areas where the majority of the available hydrogen is in atomic form and the second is produced in environments in which the hydrogen is predominantly in molecular form. The 2165 cm^{-1} (4.619 μm) band is attributed to the CN stretch in an unidentified ice constituent designated X(CN). The initial assignment to a nitrile (-C≡N) or iso-nitrile (C≡N-) has been recently questioned and the suggestion made that it is due to the CN stretch in the ion OCN^-. Although the 1670 cm^{-1} (5.99 μm) feature is due mainly to the HOH bend in H_2O, source-to-source profile variations on the high frequency side of the absorption band are attributed to organic carbonyls, implying the presence of ketones, aldehydes, esters, and carboxylic acids. The 1470 cm^{-1} (6.80 μm) band is largely attributed to the CH deformation modes of aliphatic hydrocarbons. While alcohols, such as methanol, are strongly implied by the currently available data, source-to-source spectral variations in this band are almost certainly due to variations in the amounts of different types of aliphatic hydrocarbons in the ices. These differences provide strong evidence that energetic processing, such as by ultraviolet photolysis and/or cosmic ray bombardment is an important and common process in the chemical evolution of grain mantles.

Experimental investigations of the photochemical and thermal evolution of laboratory analogs containing H_2O, CH_3OH, NH_3, CO, and saturated hydrocarbons were also described. These experiments, relevant to both interstellar and cometary ices, are the first in which CH_3OH is a major constituent. Ultraviolet photolysis of these analogs invariably produces H_2CO, CO_2, CO, CH_4, and HCO, largely at the expense of photolyzed CH_3OH. Photolysis also produces a mixture of more complex molecules, some of which contain nitrile or iso-nitrile and carbonyl groups. Most of the parent ice molecules sublime upon warm-up to 200 K, leaving behind a mixture of refractory substances. Warm-up to 250 K

liberates a component rich in $-CH_3$ groups which may correlate with the carrier(s) of the C=O and C≡N bonds. A residue rich in $-CH_2-$ groups remains even after warm-up to 300 K. The final residue is rich in $-CH_2-$ groups, independent of the $-CH_2-/-CH_3$ ratio of the hydrocarbons in the parent ice and residue components of intermediate volatility. The infrared spectrum of dust towards the galactic center, dust which is probably highly photoprocessed, shows that it is $-CH_2-$ rich, whereas the emission spectrum from Comets Halley and Wilson, which is presumably much less processed, implies that $-CH_3$ rich organics are present.

REFERENCES

A'Hearn, M. F., Hoban, S., Birch, P. V., Bowers, C., Martin R., and Klinglesmith III, D. A. (1986). Nature, 324, 649-651.

Agarwal, V. K., Schutte, W., Greenberg, J. M., Ferris, J. P., Briggs, R., Connor, S., van de Bult, C. E. P. M., and Baas, F. (1985). Origins of Life, 16, 21-40.

Allamandola, L. J. (1984). In Galactic and Extragalactic IR Spectroscopy, (M. Kessler and P. Phillips, eds.), D. Reidel, Dordrecht, pp. 5-35.

Allamandola, L. J., Sandford, S. A., and Wopenka, B. (1987). Science, 237, 56-59.

Allamandola, L. J., Tielens, A. G. G. M., and Barker, J. R. (1985). Astrophys. J. 290, L25-L28.

Allamandola, L. J., Sandford, S. A., and Valero, G. J. (1988). Icarus, submitted.

Allamandola, L. J., and Sandford, S. A. (1988), in Dust in the Universe, (D. A. Williams and M. E. Bailey eds.), Cambridge University Press, Cambridge, in press.

Allen, D. A. and Wickramasinghe, D. T. (1981). Nature, 294, 239-240.

Baas, F., Geballe, T.R., and Walther, D. M. (1986). Astrophys. J., 311, L97-L101.

Brown, P. D. (1988) in Dust in the Universe, (D. A. Williams and M. E. Bailey), Cambridge University Press, Cambridge, in press.

Calvert, J. G., and Pitts, J. N., Jr. (1966). Photochemistry, John Wiley and Sons, New York.

Capps, R. W., Gillett, F. C., and Knacke, R.F. (1978). Astrophys. J. 226, 863-868.

d'Hendecourt, L. B., and Allamandola, L. J. (1986). Astron. Astrophys. Suppl. Ser., 64, 453-467.

d'Hendecourt, L. B., Allamandola, L. J., and Greenberg, J. M. (1986). Astron. Astrophys., 152, 130-150.

d'Hendecourt, L. B., Allamandola, L. J., Grim, R. J. A., and Greenberg, J. M. (1986). Astron. Astrophys., 158, 119-134.

Danks, A. C., Encrenaz, T., Bouchet, P., Lew Bertre, T., and Chalabaev, A. (1987). Astron. Astrophys., 184, 329-332.

Day, K. L. (1979). Astrophys. J., 234, 158-161.

Delsemme, A. H., and Miller, D. C. (1971). Planet. Space Sci. 19, 1259-1274.

Duley, W. W., and Williams, D. A. (1981). Mon. Not. R. Astron. Soc., 196, 269-274.

Eiroa, C., and Hodapp, K. W. (1988). In Dust in the Universe, (D. A. Williams and M. E. Bailey, eds.), Cambridge University Press, Cambridge, in press.

Geballe, T. R. (1986). Astron. Astrophys., 162, 248-252.

Geballe, T. R., Baas, F., Greenberg, J. M., and Schutte, W. (1985). Astron. Astrophys., 146, L6-L8.

Greenberg, J. M. (1977). In Comets, Asteroids, and Meteorites, (A. H. Delsemme, ed.), University of Toledo Press, Toledo, pp. 491-497.

Grim, R. J. A., and Greenberg, J. M. (1987). Astrophys. J., 321, L91-L96.

Hagen, W., Allamandola, L. J., and Greenberg, J. M. (1979). Astrophys. Spa. Sci., 65, 215-240.

Hagen, W., Tielens, A. G. G. M., and Greenberg, J. M., (1981). Chem. Phys., 56, 367-379.

Hagen, W., Tielens, A. G. G. M., and Greenberg, J. M. (1983). Astron. Astrophys. Suppl. Ser., 51, 389-416.

Hayatsu, R., and Anders, E. (1981). Topics of Current Chemistry 99, 1-37.

Hecht, J. H., Russell, R. W., Stephens, J. R., and Grieve, P. R. (1986). Astrophys. J., 309, 90-99.

Huebner, W. F., Boice, D. C., and Sharp, C. M. (1987). Astrophys. J. 320, L149-L152.

Irvine, W. M., Schloerb, F. P., Hjalmarson, A., and Herbst,, E. (1985). In Protostars and Planets II, (D. C. Black and M. S. Matthews, eds.), Univ. Ariz. Press, Tucson, pp. 579-620.

Jiang, G. J., Person, W. B., and Brown, K. G. (1975). J. Chem. Phys., 62, 1201-1211.

Jones, T. J., Hyland, A. R., and Allen, D. A. (1983). Mon. Not. R. Astron. Soc. 205, 187-190.

Khare, B. N., Thompson, W. R., Murray, B. G. J. P. T., and Sagan, C. (1988) Icarus, in press.

Knacke, R. F., Brooke, T. Y., and Joyce, R. R. (1986). Astrophys. J. 310, L49-L53.

Knacke, R. F., and Krätschmer, W. (1980). Astron. Astrophys., 92, 281-288.

Koike, C., Hasegawa,, H., Asada, N., and Hattori, T. (1981). Astrophys. Spa. Sci., 79, 77-85.

Lacy, J. H., Baas, F., Allamandola, L. J., Persson, S.E., McGregor, P. J., Lonsdale, C. J., Geballe, T. R., and van der Bult, C. E. P., (1984). Astrophys. J., 276, 533-543.

Larson, H. P., Davis, D.S., Black, J. H., and Fink, U. (1985). Astrophy. J., 299, 873-880.

Leger, A., and Puget, J. L. (1984). Astron. Astrophys., 137, L5-L8.

Leger, A., Gauthier, S., Defourneau, D., and Rouan, D. (1983). Astron. Astrophys., 117, 164-169.

McKeegan, K. D., Walker, R. M., and Zinner, E., (1985). Geochim. Cosmochim. Acta, 49, 1971-1987.

Millar, T. J. (1988). In Dust in the Universe, (D. A. Williams and M. E. Bailey, eds.), Cambridge University Press, Cambridge, in press.

Moore, M. H., Donn, B., Khanna, R., and A'Hearn, M. F. (1983). Icarus, 54, 388-405.

Sandford, S. A., and Allamandola, L. J. (1988). Icarus, submitted.

Sandford, S. A. (1986). Science, 231, 1540-1541.

Sandford, S. A., and Walker, R. M. (1985). Astrophys. J., 291, 838-851.

Sandford, S.A., Allamandola, L. J., Tielens, A. G. G. M., and Valero, G. J., (1988). Astrophys. J., in press (June 1, 1988).

Schutte, W. A. (1988). Ph. D. Dissertation, Leiden University.

Strazzulla, G. (1985). Icarus, 61, 48-56.

Strazzulla, G., Cataliotti, R. S., Calcagno, L., and Foti, G. (1984). Astron. Astrophys., 133, 77-79.

Swan, P., Walker, R. M., Wopenka, B., and Freeman, J. J. (1987). Meteoritics 22, 510-511.

Tielens, A. G. G. M., and Hagen, W. (1982). Astron. Astrophys., 114, 245-260.

Tielens, A. G. G. M., and Allamandola, L. J. (1987). In Physical Processes in Interstellar Clouds, (G. E. Morfill and M. Scholer, eds.), D. Reidel, Dordrecht, pp. 333-376.

Tielens, A. G. G. M., Allamandola, L. J., Bregman, J. D., Witteborn, F. C., Wooden, D., and Rank, D. M. (1988). Astrophys. J., submitted.

Tokunaga, A. T., Smith, R. G., Nagata, T., DePoy, D. L., and Sellgren, K. (1986). Astrophys. J. 310, L45-L48.

Tomeoka, K., and Buseck, P. R. (1986). Science, 231, 1544-1546.

Whittet, D. C. B. (1988). In Dust in the Universe, (D. A. Williams and M. E. Bailey, eds.), Cambridge University Press, Cambridge, in press.

Whittet, D. C. B., Longmore, A. J., and McFadzean, A. D. (1985). Mon. Not. R. Astro. Soc., 216, 45p-50p.

Wickramasinghe, D. T., and Allen, D. A. (1986). Nature, 323, 44-46.

Williams, D. A. (1988). In Dust in the Universe, D. A. Williams and M. E. Bailey eds.), Cambridge University Press, Cambridge, in press.

Williams, D. A. (1987). In Physical Processes in Interstellar Clouds, (G. E. Morfill and M. Scholer, eds.), D. Reidel, Dordrecht, pp. 337-388.

Willner, S. P., Puetter, R. C., Russell, R. W., and Soifer, B. T. (1980). In Interstellar Molecules, (B. H. Andrew, ed.), D. Reidel, Dordrecht, pp. 381-386.